

Some studies on Heat-Affected Zone (HAZ) Toughness behavior of API 5L X52 steel

Ashish Kumar^{1,2}, Santosh Kumar^{1,2}, Rajneesh Kumar¹

¹National Metallurgical Laboratory, Jamshedpur.

²National Institute of Technology, Warangal.

Corresponding author: rkgupta@nmlindia.org

ABSTRACT

Heat Affected Zone (HAZ) simulation by Gleeble is a useful method for evaluating welding process parameters to improve the toughness of weld HAZ by optimizing process parameters. The HAZ Toughness in low alloy steels is strongly influenced by the welding parameters (as HAZ microstructure is influenced by the heat input and cooling rate). In the present work different regions of weld HAZ of API 5L X52 steel have been simulated by using Gleeble @ 3800 Thermal- Mechanical Simulator. Two cooling rates ($t_{8/5}$) 10 s to simulate low heat input (LHI) welding conditions without preheating, ($t_{8/5}$) 40s to simulate high heat input (HHI) welding were used. Charpy V-notch impact tests were conducted on the simulated as well as on the base material at room temperature (25° C) and at -40° C. Results showed that HHI simulated coarse grain HAZ (CGHAZ) region attributed highest Impact energy of 300 J in comparison to 199 J of base material at 25° C. In HAZ regions, lowest room temperature toughness was observed in sub critical HAZ (SCHAZ) for both HHI and LHI conditions. Lowest impact energy at -40° C was observed in fine grained HAZ (FGHAZ) for both HHI and LHI conditions. Hardness test showed that LHI samples exhibited slightly higher hardness than HHI condition and the hardness profile for HAZ regions was similar for both HHI and LHI conditions.

1.0 INTRODUCTION

The development of high strength steels for line pipe applications possess great demands because these steels are required to resist the initiation and propagation of cracks in order to avoid fracture. From the mid 1960's, various classes of HSLA steels have been used for gas and oil transportation. API 5L X52 steel was one of the earliest classes of line pipe steels with a microstructure consisting of mainly ferrite and pearlite [1]. The oil, gas and petrochemical industries have been using API 5L X52 pipes and other similar materials for off-shore and onshore applications [2]. During the construction of pipelines, welding of smaller pieces of pipes is being performed. The region near to the weld metal known as HAZ (heat affected zone), possess poor toughness because of reheating taken

place below the solidus temperature. Many studies have shown that the loss in toughness always happens in weld heat affected zone (HAZ) and fracture typically occurs in the weld metal or the heat-affected zone (HAZ) rather than in the base material [3]. To prevent catastrophic service failure, it is necessary to study the effect of welding thermal cycles on weld HAZ toughness and determine optimum welding conditions. So the present work was undertaken to study the toughness behavior in weld HAZ. Though it is difficult to analyze the toughness behavior in the sub zones of the HAZ (CGHAZ, FGHAZ, ICHAZ, and SCHAZ) because HAZ region in welded joint is narrow and are more heterogeneous. But this difficulty can be overcome by doing simulation of HAZ on GLEEBLE (thermo mechanical simulator). The weld HAZ toughness relies

on the microstructure present in those regions because the microstructural development in the HAZ during welding depends on the chemical composition of steel and also the employed thermal cycle [4, 5]. Microstructure further depends on weld heat input conditions, which have a direct influence on the peak temperature and cooling rate of the weld thermal cycle [6].

2.0 MATERIALS AND EXPERIMENTAL DETAILS

2.1 Materials

The experimental materials evaluated in this present work included API 5L X52 steel and mild steel. 12 mm thick rolled plate of API 5L X52 steel was used for preparing Gleeble simulation specimens. Due to limited availability of X52 material, mild steel plates of thickness 10 mm cut from a long plate were used for making test welds. The chemical analysis of materials was carried out using DRS method and is given in **Table 1**.

2.2 Theoretical calculation for Peak Temperatures and Cooling Rates

Various regions are formed in weld HAZ due to variation in thermal cycles experienced in these regions causing variation in the resulting microstructure. These thermal cycles can be fairly constructed if someone knows peak Temperature and the

cooling rate ($t_{8/5}$). The cooling time in sec from temperature 800°C to 500°C ($t_{8/5}$) is important in steels due to transformation microstructure point of view. Peak temperature and cooling rates can be calculated at different regions on weldment from weld center line by using the equation given below [7].

$$\frac{1}{T_p - T_o} = \frac{\sqrt{2\pi p e C h y}}{H_{net}} + \frac{1}{T_m - T_o}$$

Where, T_p = The Peak Temperature in °C at a distance, y (mm) from the weld fusion boundary. (The peak temperature equation does not apply at points within the weld metal but only in the adjacent HAZ), T_m = Melting temperature in degree centigrade, C = Specific heat capacity, H = Heat input, e = 2.718 base of the natural logarithmic.

Cooling Rate can be calculated at different regions on weldments from weld center line by the following equation [7].

$$R = \pi p k C \left(\frac{h}{H_{net}}\right)^2 (T_c + T_o)^3$$

Where, h = thickness of the plate (mm), C = specific heat capacity of base metal (J/g °C), K = thermal conductivity of base metal (J/mm s °C), T_c = temperature at which cooling rate calculated (°C), T_o = initial plate temperature (°C).

Table 1 : Chemical composition (wt %) of base metals and filler Wire

Material	C	Mn	Mo	Cr	V	Nb	S	P	Si	Cu
API 5L X52	0.133	0.811	0.0078	0.031	0.005	0.0005	0.011	0.018	0.0019	–
Mild Steel	0.16	1.51	0.007	0.029	0.082	0.0005	0.023	0.027	–	–
SAW Wire	0.10	1.2	0.50	–	–	–	0.018	0.018	0.10	0.25

Table 2 : Calculated values of Peak Temperatures and cooling rates at different regions of weld

Distance from center line(mm)	1	2	3	10	15	20
Peak temperature (°C)	1381.784	1134.37	768.432	633.469	490.605	402.071
Distance from center line(mm)	1	2	3	10	15	20
Cooling Rate (°C/sec)	59.850	40.710	28.934	5.370	2.406	1.278

2.3 Preparation of test weld

Simulation of HAZ of submerged arc welds (SAW) of API 5L X52 steel was the objective of the study. Test welds were made by SAW process to record thermal cycle experienced at various distances from weld centre line during welding. The purpose of making test welds was to record the thermal cycles to compare acquired thermal cycles with the computed thermal cycles. Due to material limitation mild steel plates were used for making weld (considering density, thermal conductivity and specific heat capacity are almost same as API 5L X52). A single bevel butt joint with root face 3 mm and bevel angle 45° was made by two mild steel plates of 10 mm thick and dimension of 300 mm in length and 100 mm in width as shown in Fig 1. The welding wire of diameter Ø3.16 mm with basic agglomerated flux was used. Chemical composition of filler wire used is given in Table 1 and the process parameters are given in Table 2. Three thermocouples were connected to the weld coupon (on the plate with square edge) at 10 mm, 15 mm and 20 mm from center line. Temperature data during welding and subsequent cooling from the thermocouples was acquired using a National Instruments data acquisition card and LabView software. The time temperature plots obtained have been shown in Fig. 2. These plots were further used to compare peak temperature and cooling rates with the theoretical computed ones as per standard equation. It was found that the computed results were in conformity with the experimental one.

2.4 HAZ Simulation by Gleeble

The primary advantages of using the Gleeble is that it is able to produce a relatively large volume of distinct microstructure in a single test sample [8]. This feature combined with precise

Table 3 : Welding parameters for SAW process

Voltage(V)	25
Current(I)	300
Welding speed (mm/sec)	3.33
Plate thickness (mm)	11
Heat input (j/mm)	2250
To (initial plate temperature)	25
Tm (melting temperature in ° C)	1600

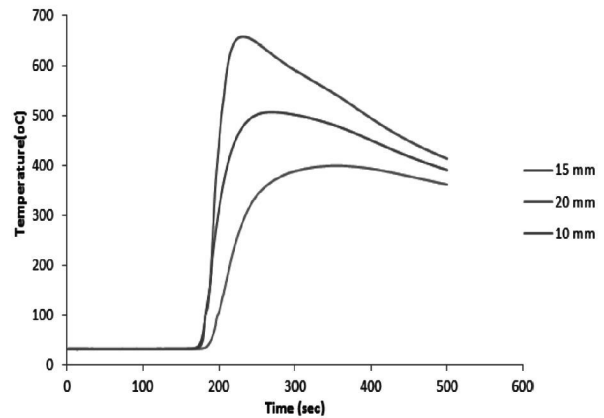


Fig 2: Temperature profile measured during test welds

temperature control allows for simulation of microstructural regions that are difficult to analyze in an actual weldments. Test samples of rectangular shape (70mm x 11mm x 11mm) API 5L X52 were used for the simulation of weld HAZ. These samples were cut keeping their length parallel to rolling direction of the plate, and machined to the size. The thermal-

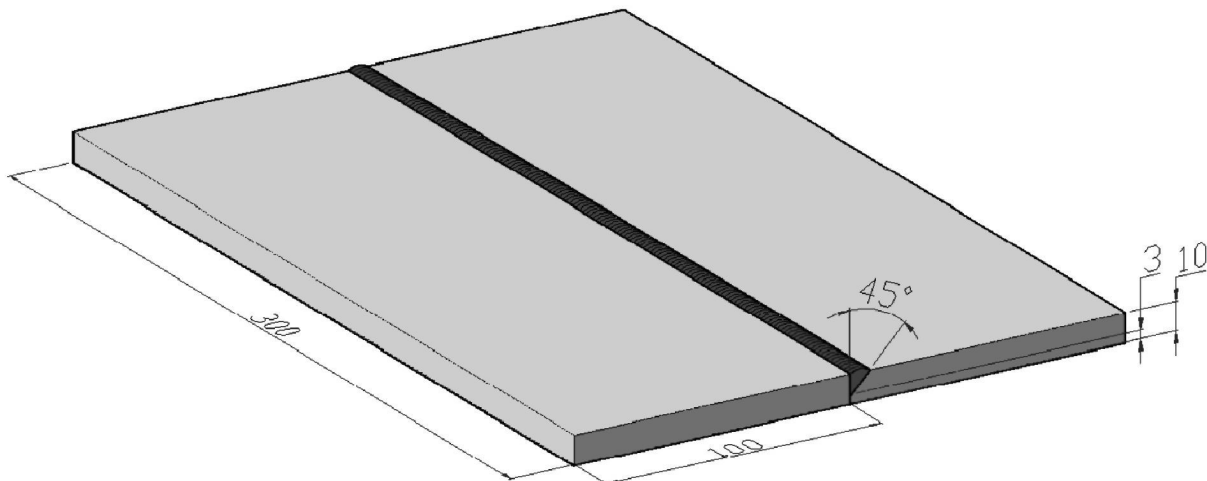


Fig 1 : Schematic view of the test weld (all dimension were described in mm).

cycle simulations were conducted with the Gleeble chamber in high vacuum of approximately 10^{-6} torr (1.3×10^{-4} Pa) to limit sample surface oxidation and thermocouple detachment. During simulation the samples were resistance heated through the low-frequency (60 Hz) alternating current to the peak temperature at a linear rate of $100 \text{ }^\circ\text{C/s}$ and held for 1 s before cooling to ambient temperature. Closed-loop temperature control is provided by a thermocouple with type K which is percussion welded at the midsection of the sample. Two weld cooling rates were simulated for each sub zone of HAZ. (i) A faster cooling rate to simulate LHI welding conditions with no preheat, and (ii) A slower cooling rate to simulate HHI welding conditions with a moderate preheat temperature. The cooling rates were achieved through the selection of grip sets. A standard copper grip set was used for the LHI simulations. For the HHI simulations, a stainless steel grip set that provided minimal contact at the ends of the sample was used. The average $t_{9/5}$ times, where $t_{9/5}$ represents the cooling time from $800 \text{ }^\circ\text{C}$ to $500 \text{ }^\circ\text{C}$, were 10 s and 43 s for the LHI and HHI simulations, respectively. The $t_{9/5}$ is a long-established index of the cooling rate of the weld thermal cycle for steels as it controls the resulting microstructure [10,11].

Table 4 : Peak Temperature experienced by the sub zones of HAZ.

HAZ Region	Location	Peak Temperature($^\circ\text{C}$)
Sub Critical HAZ	T \square A ₁	650
Inter Critical HAZ	A ₂ \square T \square A ₃	750
Fine Grain HAZ	T \square A ₃	950
Coarse Grain HAZ	T \square \square A ₃	1300

Table 4 provides peak temperature of various sub zones of HAZ. Based on peak temperature and computed cooling rates for different heat input thermal cycles were constructed to be simulated in Gleeble. For extrapolating cooling rate beyond $t_{9/5}$ range following exponential equation was used:

$$T = T_{\max} e^{-0.47/\Delta t}$$

Where,

T_{\max} = Peak Temperature,

Δt = Cooling time (800-500),

t = time (sec).

The Thermal Cycle for each sub region of HAZ for LHI and HHI which was used in Gleeble are shown in **Fig 3**.

2.5 Charpy Impact toughness testing

The toughness of simulated HAZ and base material specimens was examined using the Charpy V-notch impact test. Standard Charpy test specimens of size (10mm x 10mm x 55mm) mm Specimens (as shown in **Fig 4**) were machined in accordance with ASTM E23. These samples were tested at an ambient temperature of ($25 \text{ }^\circ\text{C}$) and at sub zero temperature ($-40 \text{ }^\circ\text{C}$). For the tests carried out at low temperature, the samples were first cooled to ($-40 \text{ }^\circ\text{C}$) by immersion in a solution of acetone and dry ice followed by hold in the solution for 20 minutes to stabilize the temperature and then promptly tested. Three specimens of each experiment condition were tested to rule out any absurd value.

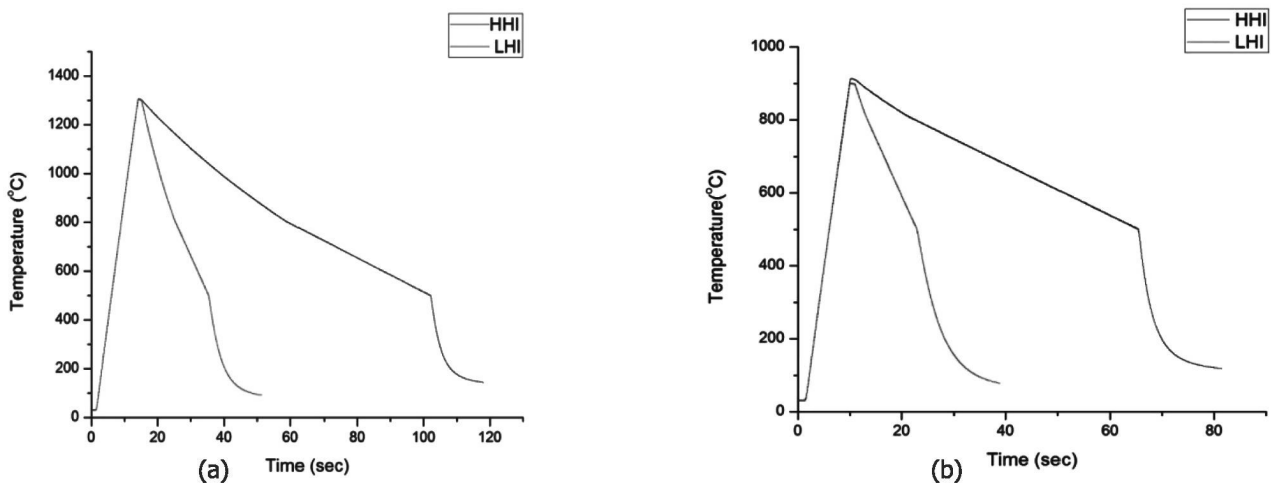


Fig 3 : Thermal cycles used in Gleeble for Simulation of (a) Coarse Grained HAZ (b) Fine Grained HAZ



Fig 4 : Standard Charpy specimens of simulated samples

2.6 Micro hardness

The Vickers hardness measurement was done on HAZ simulated samples and base material using a LECO M-400-H1 hardness testing machine with a load applied 1kg in accordance with ASTM E 384-10.

2.7 Scanning Electron Microscopy

Scanning Electron Microscope was used to analyze the fracture surface in this present work. For fractography analysis, the fracture surfaces of impact tested samples were cut followed by ultrasonic cleaning with methanol and dried. The sample with fracture surface was mounted on a small aluminum stage using conductive carbon cement, and then was placed in the SEM chamber for analyzing.

2.8 Optical Microscopy

Light optical microscopy is one of the most commonly used techniques for microstructure characterization. The optical microscope used for the present investigations was LEICA DM2500M. HAZ simulated specimens were cut in direction along with their length keeping rolling direction perpendicular to the cross section. The samples were mounted in bakelite and then grounded on abrasive papers of grade 100, 270, 500 and 1000. Thereafter these were polished to a mirror like surface finally by cloth polishing with alumina. The samples were etched by using 2% nital before examination under microscope.

3.0 RESULTS AND DISCUSSION

Impact toughness

The Impact energy vs. different regions of HAZ plots at 25 °C and -40 °C are shown in Fig. 5. The simulated HAZ sample showed to have better impact toughness than the BM at both test temperatures, suggesting that there is no toughness loss in the weld HAZ regions. HHI simulated Coarse Grain HAZ region was having highest impact energy of 300 J in comparison to 199 J of base material at 25 °C. In HAZ regions, lowest room temperature toughness was observed in SCHAZ for both HHI and LHI conditions. Lowest impact energy at -40 °C was observed in fine grained FGHAZ for both HHI and LHI conditions. At -40 °C LHI HAZ samples were found having higher impact energy than HHI HAZ samples. Higher toughness for the HAZ regions at low temperatures than base metal can be partially attributed to the formation of retained austenite in the HAZ microstructures, which has been shown to have a beneficial effect on toughness. The effect of retained austenite has been attributed to acting as a sink for elements deleterious to fracture toughness such as carbon, and in disrupting the crystallographic alignment of the martensite packets. Thermally steady austenite that is formed along martensite lath boundaries acts to interrupt the crystallographic alignment of the laths within the martensite packets, preventing cooperative trans-packet cleavage. The lower impact values of the BM could indicate a lower than expected volume fraction of austenite or the constant presence of cementite in the microstructure. The overall results suggest

that the liquid nitrogen quench intended to form precipitated austenite in the BM are not necessary to obtain adequate properties.

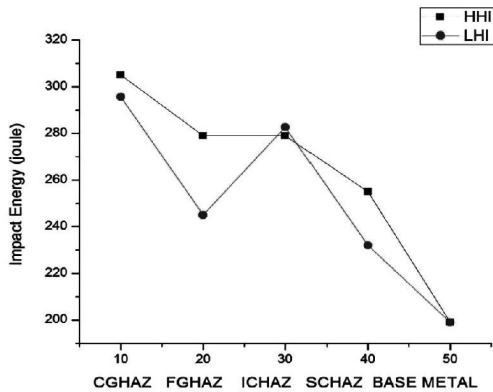


Fig 5a : Impact Energy of different HAZ regions for HHI and LHI at 25 ° C

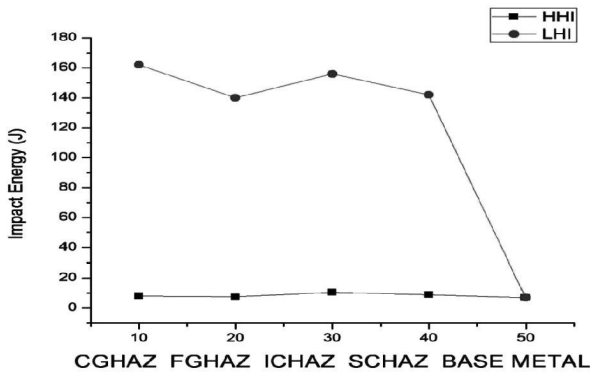


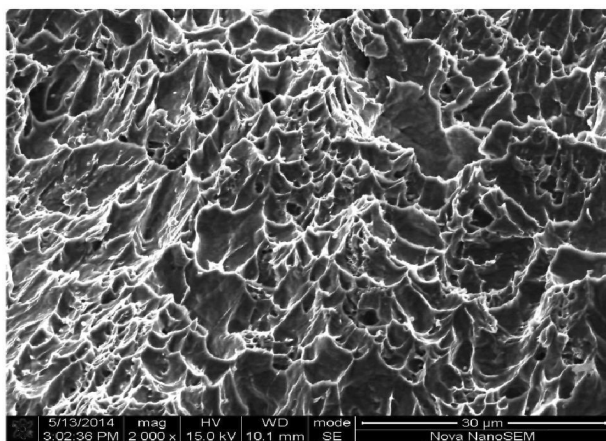
Fig 5b : Impact Energy of different HAZ regions for HHI and LHI at -40 ° C

Fractography

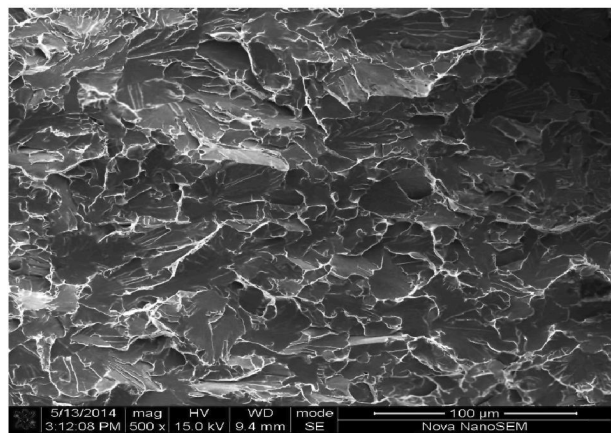
The fracture surface of HHI simulated HAZ impact specimens as observed in SEM have been shown in Fig. 6. The fracture surface of impact tested sample at room temperature (25 ° C) exhibited a ductile tearing morphology. The fracture appears to be predominantly intergranular with some grain facets exhibiting ductile tearing features. In the fractograph of the impact specimen, tested at lower temperatures (-40 ° C) dominant quasi-cleavage fracture mode was observed.

Metallography

Fig. 7 shows optical micrographs of the base metal and HAZ simulated specimens observed at 500x. Base material microstructure consisting of typical ferrite, pearlite structure as shown in Fig 7a. From Fig 7b CGHAZ of LHI condition sample posses a small volume fraction of widmansatten ferrite with Lath martensite and ferrite non aligned with secondary phase was observed. The HHI condition CGHAZ simulated sample having predominantly widmanstatten ferrite with bainite and pearlite structures can be seen in Fig 7c. Uniformly distributed polygonal ferrite in lath martensite matrix was found in FGHAZ of LHI condition simulated sample from Fig 7d. Whereas for FGHAZ of HHI condition simulated sample posses primary ferrite along with grain boundaries (GF) with large volume fraction of bainitic structures can be seen in Fig 7e. For ICHAZ region LHI condition simulated sample having fine interlocking microstructure of intragranular (acicular ferrite) with small volume fraction of bainitic structure from Fig 7f. While bainitic structures with surrounding lath martensite, polygonal ferrite was prevail for ICHAZ of HHI condition simulated sample in Fig 7g. It was observed that SCHAZ of LHI condition simulated sample posses similar microstructure in comparison to the base material having ferrite, pearlite structures from Fig 7h.



(a)



(b)

Fig 6: fracture surface of HHI HAZ impact test specimen (a) at room temperature (b) at -40o C

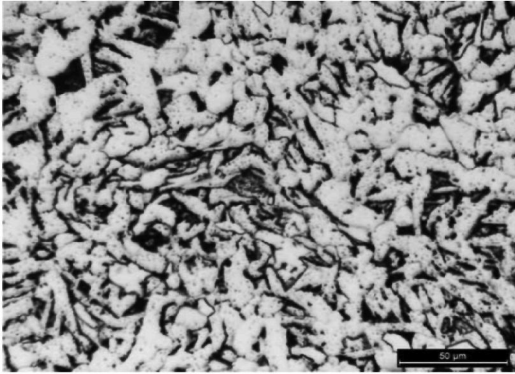


Fig 7a : Base material at a magnification of 500x

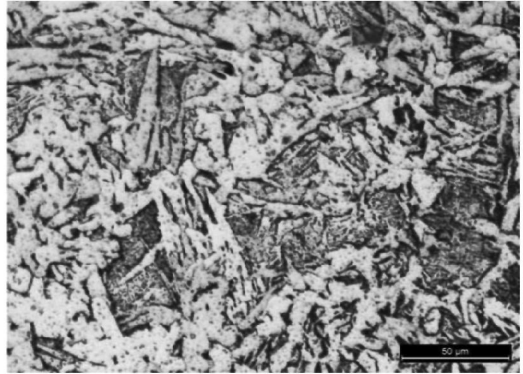


Fig 7b : CGHAZ (LHI) at a magnification of 500x

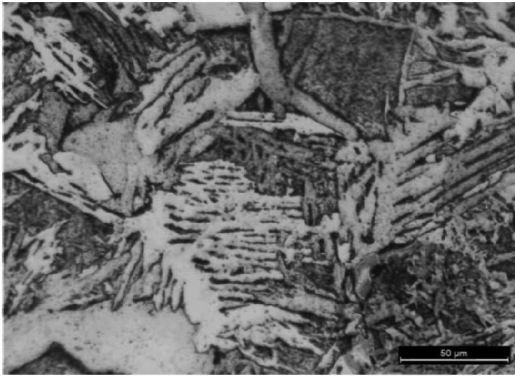


Fig 7c : CGHAZ (HHI) at a magnification of 500x

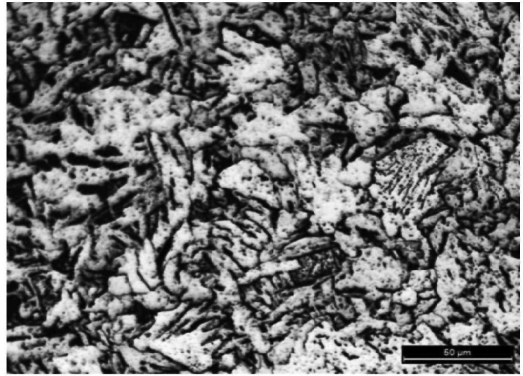


Fig 7d : FGHAZ (LHI) at a magnification of 500x



Fig 7e : FGHAZ (HHI) at a magnification of 500x

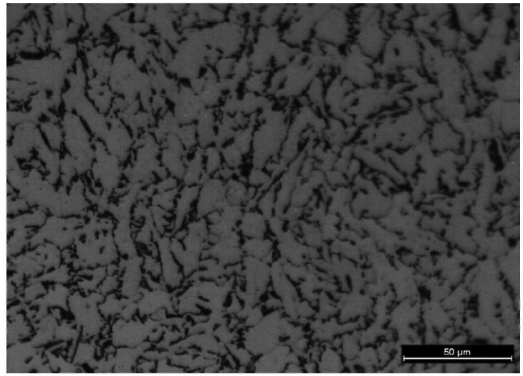


Fig 7f : ICHAZ (HHI) at a magnification of 500x

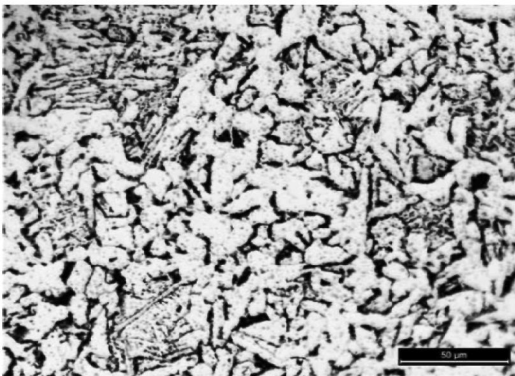


Fig 7g : ICHAZ (LHI) at a magnification of 500x

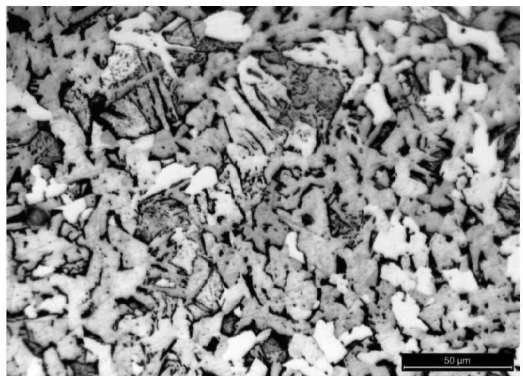


Fig 7h : SCHAZ (LHI) at a magnification of 500x

Microhardness

Micro hardness values observed in base metal and in various HAZ specimens have been given in **Table 5**.

Table 5 : Micro Hardness values at different regions on HAZ.

Different Regions	Average Vickers values (HV)
Base material	196
CGHAZ (HHI)	171
CGHAZ (LHI)	176
FGHAZ (HHI)	174
FGHAZ (LHI)	182
ICHAZ (HHI)	229
ICHAZ (LHI)	241
SCHAZ (HHI)	205
SCHAZ (LHI)	209

A plot of Vickers micro hardness of different HAZ regions in respective of their location from fusion line has been shown in Figure 8 for both the heat input conditions. It is clear that the Vickers hardness plots for the different HAZ regions exhibit similar trend for both the LHI and HHI conditions with a slightly higher hardness observed in the LHI samples for each HAZ region. A hardness peak was observed in the ICHAZ with the lowest hardness occurring in the CGHAZ.

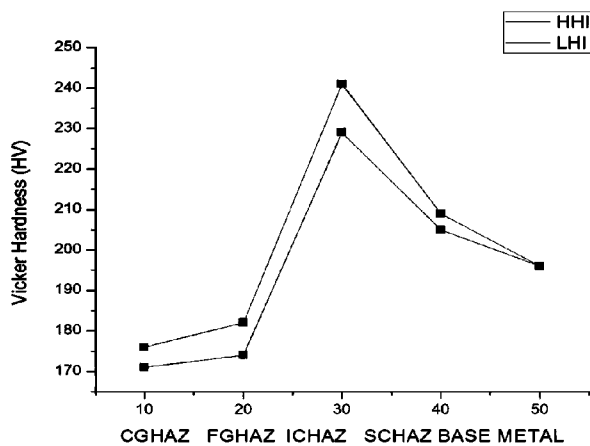


Fig 8 : Vickers hardness across the different regions of HAZ for HHI and LHI

4.0 CONCLUSIONS

- HAZ regions exhibited higher toughness than the BM at both test temperatures of 25°C and -40°C.
- Among all HAZ regions CGHAZ region showed highest toughness for both the heat inputs. The highest toughness at both temperatures was exhibited by the CGHAZ (HHI), with toughness values of 300 J at 25°C.
- Among all HAZ regions minimum hardness was observed in CGHAZ region of both HHI weld (171 HV) and LHI weld (176 HV). Base metal hardness was 196 HV.
- The Fractographic analysis of all impact specimens tested at 25°C exhibited predominantly ductile micro void coalescence fracture while specimens tested at -40°C exhibited quasi-cleavage fracture.

ACKNOWLEDGEMENT

Authors are grateful to Director, CSIR-National Metallurgical Research Laboratory to permit publishing of this work.

REFERENCES

- Tamehiro H, Asahi H, Hara T, and Terada Y "Ultra-high Strength, Weldable Steels with Excellent Ultra-low Temperature Toughness" United States Patent 6264760, EXXON Production Research Company and NIPPON Steel, 1999.
- Perdomo JJ, Gonzalez JJ and Viloria A "Corrosion of API 5L and X52 in Crude Oil/Water/Gas Mixtures" Materials Performance, 2000; 39: 76-79.
- Gaudet MJ "Mechanical behavior and fracture properties of the heat affected zone for dual torch welded X80 steel" Thesis, The University of British Columbia, 2010.
- Yapp D and Blackman S "Recent developments in high productivity pipeline welding" Journal of the Brazilian Society of Mechanical Sciences and Engineering, 2004; 26: 89-97.
- Fairchild DP "High strength steels beyond X80" in Proceedings of pipe dreamer's conference, Application and evaluation of high-grade line pipes in hostile environments, Yokohama, Japan, 2002.
- Lippold J "Recent Developments in Weldability Testing, Hot Cracking Phenomena in Welds", edited by T. Bollinghaus and H. Herold, Springer-Verlag Germany, 2005, pp. 271- 290.
- Olson DL, Siewert TA, Liu S and Edwards GR, "Welding Brazing and Soldering" ASM International, 1993.
- Gleeble 3800 System - Product Description and Specifications, technical literature, Dynamic Systems Inc., Poestenkill, NY, 2006, pp.10-19.
- Bibliography of Gleeble Papers, tech. rep., Dynamic Systems Inc., Poestenkill, NY 2006.
- Caron, J. "Weldability Evaluation of Naval Steels" PhD Thesis, The Ohio State University, 2010.
- Easterling K "Introduction to the Physical Metallurgy of Welding" UK: Oxford, 1992.